HHS Public Access

Author manuscript

Neuropsychopharmacology. Author manuscript; available in PMC 2010 February 01.

Published in final edited form as:

Neuropsychopharmacology. 2009 August ; 34(9): 2112–2124. doi:10.1038/npp.2009.36.

Selective Alterations in Postsynaptic Markers of Chandelier Cell Inputs to Cortical Pyramidal Neurons in Subjects with Schizophrenia

Dianne A. Cruz, M.S.[1,*], **Cassandra Weaver, B.A.**[1], **Emily M. Lovallo, B.S.**[2], **Darlene S. Melchitzky, M.S.**[1,3], and **David A. Lewis, M.D.**[1,2]

[1]Department of Psychiatry, University of Pittsburgh, Pittsburgh, PA

[2]Department of Neuroscience, University of Pittsburgh, Pittsburgh, PA

[3]Department of Biology, Mercyhurst College, Erie, PA

Abstract

Markers of GABA neurotransmission between chandelier neurons and their synaptic targets, the axon initial segment (AIS) of pyramidal neurons, are altered in the dorsolateral prefrontal cortex (dlPFC) of subjects with schizophrenia. For example, immunoreactivity for the GABA membrane transporter (GAT1) is decreased in presynaptic chandelier neuron axon terminals, whereas immunoreactivity for the $GABA_A$ receptor α2 subunit is increased in postsynaptic AIS. To understand the nature and functional significance of these alterations, we determined the density, laminar distribution and length of AIS immunoreactive for ankryin-G and βIV spectrin, two proteins involved in the regulation of synapse structure and ion channel clustering at AIS, in dlPFC area 46 from 14 matched triads of subjects with schizophrenia or major depressive disorder (MDD) and normal comparison subjects. The density of ankyrin-G-immunoreactive (IR) AIS in the superficial, but not in the deep, cortical layers was significantly decreased by 15-19% in the subjects with schizophrenia relative to the other subject groups. In contrast, no group differences were present in the density of βIV spectrin-IR AIS. The length of labeled AIS did not differ across subject groups for either ankyrin-G or βIV spectrin. The density of ankyrin-G-IR AIS was not altered in the dlPFC of macaque monkeys chronically exposed to antipsychotic medications. Given the important role of ankyrin-G in the recruitment and stabilization of sodium channels and other integral membrane proteins to AIS, our findings suggest that these processes are selectively altered in superficial layer pyramidal neurons in subjects with schizophrenia.

Corresponding Author: David A. Lewis, M.D., Department of Psychiatry, University of Pittsburgh, 3811 O'Hara Street, W1651 BST, Pittsburgh, PA 15213, Phone: (412)-624-3934, Fax: (412)-624-9910, E-mail: lewisda@upmc.edu.

*Current affiliation: Department of Psychiatry, University of Texas Health Science Center at San Antonio

Disclosure/Conflicts of Interest David A. Lewis currently receives investigator-initiated research support from the BMS Foundation, Bristol-Myers Squibb, Curridium Ltd and Pfizer and in 2007-2009 served as a consultant in the areas of target identification and validation and new compound development to AstraZeneca, Bristol-Myers Squibb, Hoffman-Roche, Lilly, Merck and Neurogen. All other authors have no conflicts of interest to disclose.

Keywords

Ankyrin-G; βIV spectrin; axon initial segment; GABA; prefrontal cortex

Introduction

Postmortem studies have revealed alterations in both pre- and post-synaptic markers of GABA neurotransmission in the dorsolateral prefrontal cortex (dlPFC) of subjects with schizophrenia. Presynaptically, levels of the mRNAs encoding 1) the 67-kilodalton isoform of glutamic acid decarboxylase (GAD_{67}), the principal enzyme responsible for the synthesis of GABA; 2) the GABA membrane transporter (GAT1); and 3) the calcium-binding protein parvalbumin (PV) are lower in schizophrenia (Volk, *et al* 2000; Volk, *et al* 2001; Hashimoto, *et al* 2003; Akbarian, *et al* 1995; Ohnuma, *et al* 1999; Guidotti, *et al* 2000; Hashimoto, *et al* 2008). These alterations are accompanied by reduced GAT1 immunoreactivity in the characteristic axon terminals (termed cartridges) of PV-containing chandelier neurons (Woo, *et al* 1998; Pierri, *et al* 1999) that form symmetric synapses onto the axon initial segments (AIS) of pyramidal neurons in the primate dlPFC (Williams, *et al* 1992; Melchitzky, *et al* 1999). Postsynaptically, immunoreactivity for the $GABA_A$ receptor α_2 subunit is increased in pyramidal neuron AIS in the dlPFC of subjects with schizophrenia (Volk, *et al* 2002). Together, these findings suggest that deficient GABA synthesis in chandelier neurons in schizophrenia, with the changes in GAT1, PV and $GABA_A$ receptors reflecting compensatory responses to augment the efficacy of GABA inputs to pyramidal neuron AIS (Lewis, *et al* 2005).

However, understanding the nature and functional significance of these alterations requires knowledge of other processes that affect GABA neurotransmission at pyramidal neuron AIS in schizophrenia. Of particular interest is whether the alterations in pre- and postsynaptic markers of GABA neurotransmission are accompanied by changes in proteins that regulate synapse structure and ion channel clustering in pyramidal neuron AIS. For example, the 480- and 270-kDa isoforms of ankyrin-G, members of a class of adaptor molecules that link various membrane proteins to the cytoskeleton, are localized to AIS (and nodes of Ranvier) of certain neurons, including cortical pyramidal neurons (Kordeli, *et al* 1995; Susuki and Rasband, 2008). In the cerebellum, ankyrin-G interacts with the neuronal cell adhesion molecule neurofascin to recruit and stabilize GABA synapses at the AIS of Purkinje cells (Ango, *et al* 2004). Binding to ankyrin G is also essential for the localization of many other membrane proteins to the AIS (Susuki and Rasband, 2008), including the voltage-gated Na^+ channels that are required for action potential generation (Zhou, *et al* 1998). In addition, the cytoskeletal protein ßIV spectrin, which is localized to the AIS of pyramidal neurons through its direct interaction with ankryin-G (Yang *et al* 2007), is a critical component in the maintenance of membrane structure and molecular organization (Lacas-Gervais, *et al* 2004), and thus the stability (Yang, *et al* 2007), of AIS.

Given the importance of these proteins in pyramidal neuron AIS structure and function, we examined human postmortem brain tissue containing dlPFC area 46 to determine whether the laminar densities of AIS immunoreactive (IR) for ankyrin-G or ßIV spectrin are altered

in subjects with schizophrenia relative to normal control subjects and subjects with major depressive disorder (MDD). We also determined 1) the impact of potential clinical confounds on these measures, 2) the length of ankyrin-G- and ßIV spectrin-IR AIS in the same subjects, and 3) the density of labeled AIS in area 46 of macaque monkeys chronically exposed to typical or atypical antipsychotic medications.

Methods

Characteristics of study subjects

Brain tissue from 42 subjects was collected during autopsies conducted at the Allegheny County Medical Examiner's Office after consent was obtained from the next-of-kin (Table 1). All procedures were approved by the University of Pittsburgh's Committee for Oversight of Research Involving the Dead and Institutional Review Board for Biomedical Research. Consensus DMS-IV diagnoses were made by an independent panel of experienced clinicians using information obtained from structured interviews with relatives and review of medical records (Glantz and Lewis, 1997). Each subject with schizophrenia was matched to one normal comparison subject and one subject with MDD on the basis of sex, and as closely as possible for age and postmortem interval (PMI), creating 14 subject triads for the purposes of tissue processing. The mean (± SD) age (comparison: 52.4 ± 8.6 years; schizophrenia: 52.6 ± 8.5 years; MDD: 53.0 ± 7.6 years; $F_{2,39}$ = .02, p = .98) and PMI (comparison: 11.8 ± 5.9 hours; schizophrenia: 13.4 ± 5.8 hours; MDD: 13.5 ± 5.7 hours; $F_{2,39}$ = .38, p = .69) did not differ across subject groups. The mean age of illness onset was 29.9 ± 9.4 years for the schizophrenia subjects and 41.6 ± 10.7 years for the MDD subjects. Neuropathological evaluations revealed no abnormalities in any subjects. This same cohort of subjects has been used in previous studies of markers of chandelier neuron axon terminals and pyramidal neuron AIS (Pierri, *et al* 1999; Volk, *et al* 2002).

Tissue processing

The left hemisphere of the brain was cut into standardized coronal blocks (~1.2 cm thick). Tissue blocks were immersed in 4% paraformaldehyde in phosphate buffer for 48 hours and stored in a cryoprotectant solution at -30°C (Cruz, *et al* 2003). Previous studies have demonstrated that storage under these conditions does not affect immunoreactivity for a number of proteins (Erickson, *et al* 1998; Pierri, *et al* 1999; Cruz, *et al* 2003). Mean tissue storage times (e.g., for the ankyrin-G immunocytochemical study, normal comparison: 135 ± 29 months; schizophrenia: 141 ± 28 months; MDD: 121 ± 34 months) did not differ ($F_{2,39}$ = 1.65, p = .206) across subject groups. Tissue blocks were sectioned (40 μm) coronally on a cryostat and a sample of equally-spaced sections through the entire block were stained for Nissl substance with thionin. The stained sections were used to identify area 46 (Fig. 1A) of the dlPFC according to cytoarchitectonic criteria (Daviss and Lewis, 1995; Rajkowska and Goldman-Rakic, 1995).

Three sets of adjacent tissue sections approximately 400 μm apart and each containing dlPFC area 46 from each subject were processed in a randomized block design (i.e., with one section from each subject in a triad always processed together and with different combinations of triads in each immunocytochemical experiment). One set of sections was

processed for ankyrin-G immunoreactivity with a mouse monoclonal IgG_1 antibody (1:200 dilution, Santa Cruz Biotechnology, Santa Cruz, CA) that recognizes the 480 and 270 kDa isoforms of the protein; the adjacent set of sections was processed for βIV spectrin immunoreactivity with a rabbit polyclonal antibody (1:750 dilution, kindly provided by Dr. Matthew Rasband, Baylor College of Medicine, Houston, TX) raised against the specific domain (SD) of βIV spectrin. Exclusion of the primary antibodies in control experiments resulted in the complete absence of immunoreactivity (data not shown). The specificity of these antibodies has been demonstrated by the absence of immunoreactivity in tissue from mice with genetic deletions of ankyrin-G (Jenkins, *et al* 2001; Jenkins and Bennett, 2001; Zhou, *et al* 1998) or βIV spectrin-SD (Yang, *et al* 2004).

To ensure adequate visualization of the proteins of interest, tissue sections were treated with an antigen retrieval procedure (Jiao, *et al* 1999) prior to primary antibody incubation. Tissue sections were placed in a .01 M sodium citrate solution (pH 8.5) at 80°C for 75 minutes, followed by a 30 minute incubation in 1% $NaBH_4$ as previously described (Cruz *et al* 2003). Sections were then 1) incubated in one of the primary antibodies for 48 hours at 4°C, 2) incubated in a biotinylated donkey anti-mouse (ankyrin-G) or a biotinylated donkey anti-rabbit (βIV spectrin) secondary antibody (1:200 dilution, Vector Laboratories, Burlingame, CA) for 1 hour at room temperature, 3) processed with a Vectastain ABC kit (Vector Laboratories) and diaminobenzidine, and 4) mounted on coded slides. The diaminobenzidine reaction product was stabilized by osmium tetroxide (Lewis, *et al* 1986), and intensified with silver nitrate and gold chloride (Pucak, *et al* 1996).

Quantification

The densities (number per mm^2) of pyramidal neuron AIS labeled with each antibody were quantified using the Stereo Investigator fractionator software (MicroBrightfield, Inc., Colchester, VT). For each section, the portion of area 46 cut perpendicular to the pial surface was identified, and two cortical zones were delineated as follows: 25% of the cortical depth immediately below the border of layers 1-2 (which corresponds to layers 2 and superficial 3) was defined as the superficial zone, and 20% of the cortical depth immediately above the layer 6-white matter border (which corresponds to layer 6) was defined as the deep zone. These cortical zones were chosen to follow the procedures used in previous studies of pre- and post-synaptic markers of GABA neurotransmission in the same subjects (Pierri, *et al* 1999; Volk, *et al* 2002). Using a 5x objective (final on screen magnification of 120x), a contour was drawn around each cortical zone and a sampling grid 300 × 300 μm (superficial) or 200 × 200 μm (deep) was placed in a random orientation over the contour. A counting frame (60 × 60 μm) within each grid square was defined as the region of quantification. For quantification of AIS immunoreactive for ankyrin-G, the mean (± SD) numbers of counting frames per section for the superficial and deep zones were 35.4 (12.3) and 60.1 (15.9), respectively. The mean (± SD) numbers of counting frames per section for βIV spectrin IR AIS in the superficial and deep zones were 37.2 (10.1) and 65.3 (19.2), respectively. As previously described, AIS were identified as intensely immunoreactive processes perpendicular to the pial surface that tapered slightly in the direction from pia to white matter (Volk *et al* 2002). With a 40x objective (final on screen

magnification of 960x), all immunoreactive AIS in the inclusion boundaries of the counting frames were identified.

One rater quantified all ankyrin-G-IR AIS (D.A.C.) and a second rater (C.L.W.) quantified all βIV spectrin-SD-IR AIS. Both raters were blind to the subject number and diagnosis of each section. Intra-rater reliability was confirmed by intra-class correlation coefficients (ICC) of .996 (95% CI = .971-.998) for ankyrin-G and .986 (95% CI = .952-.996) for βIV spectrin-SD. Inter-rater reliability between D.A.C. and C.L.W. for each type of labeled AIS was confirmed with an ICC of .992 (95% CI = .971-.980).

The lengths of ankyrin-G- and βIV spectrin-SD-immunoreactive AIS were analyzed with the Neurolucida software (MicroBrightfield, Inc.) using a 100x, NA1.4, oil immersion objective. One section from each of the normal comparison and schizophrenia subjects was used for AIS length analysis. For both ankyrin-G and βIV spectrin-SD, 20 immunoreactive AISs in the superficial cortical zone were randomly selected, traced on a video monitor at a final magnification of 2400x, and the length of the labeled AIS was determined.

Effects of antipsychotic medications

To assess the potential influence of antipsychotic medications on the density of ankyrin-G-IR AIS, we studied 18 male macaque monkeys (*Macaca fascicularis*) that had been chronically exposed to haloperidol, olanzapine, or placebo as previously described (Dorph-Petersen, *et al* 2005). All procedures were approved by the University of Pittsburgh's Institutional Animal Care and Use Committee. After approximately 2 years of treatment, monkeys were euthanized in triads (composed of one animal from each treatment group), the brain was removed and tissue blocks containing the dlPFC were placed into cold 4% paraformaldehyde for 48 hours and stored in cryoprotectant at -30°C. Two tissue sections (40 μm) per subject containing area 46 were processed for immunocytochemistry, and the densities of ankyrin-G-IR AIS were determined, using the same procedures described above for the human subjects. One rater quantified all the ankyrin-G-IR AIS (E.M.L.). The slides were coded so the rater was blind to the subject number and treatment of each specimen. The intra-rater reliability of AIS counts was confirmed by intraclass correlation coefficients (ICC) of .993 (95% CI = .946-.999). The inter-rater reliability (with D.A.C.) of AIS counts resulted in an ICC of .983 (95% CI = .941-.995).

Statistical analyses

The density of labeled AIS per subject was calculated as the average density of the three tissue sections. Two statistical models were used to test for effect of diagnosis in each cortical zone. In the first approach (Model 1), analyses of variance (ANOVA) were performed with mean density of labeled AIS as the dependent variable, diagnostic group as the main effect, and subject triad as a blocking factor. Because triads were used primarily to reduce experimental variance across groups, and did not fully control for potential differences in age, PMI or tissue storage time, we also used ANCOVA to test for a main effect of diagnosis, including sex, age, PMI and tissue storage time as covariates (Model 2). Age and tissue storage time were not significant in any of the initial analyses, so these covariates were omitted from the final analyses. Results of both statistical models are

reported. The Least Significant Difference post-hoc test was used to assess differences between diagnostic groups based on the Model 1 results.

The effect of sex, use of antipsychotic drugs, antidepressant drugs or benzodiazepines at time of death, history of alcohol and/or substance use disorder, and cause of death on the difference in AIS-IR density between matched schizophrenia-normal comparison subject pairs and MDD-normal comparison subject pairs were analyzed with ANCOVAs using sex and PMI as covariates. To determine if the densities of ankyrin-G-IR AIS and βIV spectrin-SD-IR AIS were correlated within subjects, a one-tailed Pearson correlation was conducted for each diagnostic category. Differences in AIS lengths between schizophrenia and normal comparison subjects were assessed with ANCOVAs using sex, age and PMI as covariates. Differences in the mean density of ankyrin-G-IR AIS across the groups of haloperidol-, olanzapine- and placebo-exposed monkeys were assessed by ANCOVA, with experimental group as main effect and subject triad as a covariate.

Photography

Photomicrographs (Figs. 1 and 2) were generated using a Zeiss Axiocam camera. Photomontages were assembled and the brightness and contrast were adjusted in Adobe Photoshop.

Results

General observations

In area 46 of human dlPFC, immunoreactivity for both ankyrin-G and βIV spectrin-SD was most prominently localized to the AIS of pyramidal neurons in layers 2-6 (Fig. 1). Ankyrin-G- and βIV spectrin-SD-IR AIS were intensely immunoreactive, vertically-oriented structures that were widest just beneath the base of unlabeled pyramidal neuron cell bodies and then became thinner with increasing distance from the cell body (Fig. 2). In all cortical layers and the subjacent white matter, ankyrin-G and βIV spectrin-SD immunoreactivity was also found in small punctate structures (Fig. 1) which most likely represent the nodes of Ranvier of myelinated axons (Jenkins and Bennett, 2002; Zhou, *et al* 1998).

Densities of ankyrin-G and βIV spectrin-SD-IR AIS

In the superficial cortical zone (Fig. 3A), the mean (±SD) density of ankyrin-G-IR AIS was significantly (Model 1: $F_{2,26} = 5.97$; $p = .007$; Model 2: $F_{2,37} = 3.63$; $p = .036$) decreased in subjects with schizophrenia (808.0 ± 224.4) by 19% relative to matched normal comparison subjects (1008.8 ± 213.8) and by 15% relative to subjects with MDD (951.6 ± 268.2). Post-hoc analysis revealed that mean ankyrin-G-IR AIS density in subjects with schizophrenia was significantly lower than in both normal comparison ($p = .003$) and MDD ($p = .02$) subjects; in contrast, the normal comparison and MDD groups did not differ ($p = .404$). In addition, across subject groups, the densities of ankyrin-G-IR AIS were significantly ($F_{1,37} = 5.72$; $p = .022$) greater in females than in males. In the deep cortical zone (Fig. 3B), the mean densities of ankyrin-G-IR AIS were lower than in the superficial zone for each subject group, but did not differ (Model 1: $F_{2,26} = 1.18$; $p = .322$; Model 2: $F_{2,37} = .91$; $p = .411$)

across the subject groups. No differences were observed between males and females in the deep cortical zone ($F_{1,37}$ = .05; p = .826)

The mean density of βIV spectrin-SD-IR AIS (Fig. 4) did not differ across subject groups in either the superficial (Model 1: $F_{2,26}$ = 1.68; p = .206; Model 2: $F_{2,37}$ = 1.06; p = .356) or deep (Model 1: $F_{2,26}$ = .49; p = .621; Model 2: $F_{2,37}$ = .84; p = .438) cortical zones. In addition, like ankyrin-G-IR AIS, the densities of βIV spectrin-SD-IR AIS were significantly greater in females than in males across subject groups in the superficial zone ($F_{1,37}$ = 8.55; p = .006) but not in the deep zone ($F_{1,37}$ = 1.41; p = .242).

The densities of ankyrin-G- and βIV spectrin-SD-IR AIS in the superficial zone were positively correlated in each subject group (normal comparison: r = .70, p = .005; MDD: r = .64, p = .014; schizophrenia: r = .52, p = .059), although the density of βIV spectrin-SD-IR AIS was greater than that for ankyrin-G-IR AIS for every subject (Fig. 5).

Effects of possible confounds

The effects of possible confounds on the group differences in the densities of ankyrin-G-IR AIS in the superficial cortical zone are shown in Figure 6A. The mean difference from the matched normal comparison subject did not significantly differ when the subjects with schizophrenia were divided into groups based on sex ($F_{1,11}$ = .025, p = .876), the use of antipsychotic ($F_{1,10}$ = 2.32, p = .159), benzodiazepine ($F_{1,10}$ = .11, p = .746) or antidepressant ($F_{1,10}$ = 1.61, p = .233) medications at the time of death, or a history of a substance use disorder ($F_{1,10}$ = .59, p = .462). Interestingly, those schizophrenia subjects on psychotropic medications at the time of death tended to have a smaller decrease in ankyrin-G-IR AIS density relative to their matched normal comparison subjects (Fig. 6A), suggesting that the use of medications might have obscured the magnitude of the decrease in ankyrin-G-IR AIS density due to the illness. The two subjects with schizophrenia who died by suicide had a much greater decrease in ankyrin-G-IR AIS density than those who died by other causes ($F_{1,10}$ = 5.73, p = .038; Fig. 6A). However, the schizophrenia subjects with a cause of death other than suicide still showed a significant (t_{11} = 2.38, p = .036) 14% decrease in ankyrin-G-IR AIS density relative to their matched comparison subjects. Finally, the density of ankyrin-G-IR AIS was similarly decreased ($F_{1,10}$ = .11, p = .758) in both “pure” schizophrenia (n = 11) and schizoaffective (n = 3) subjects.

For the subjects with MDD (Fig. 6B), the mean difference from their matched normal comparison cases in the density of ankyrin-G-IR AIS in the superficial zone did not significantly differ when MDD subjects were divided on the basis of sex ($F_{1,11}$ = 1.53, p = .243), the use of antipsychotic ($F_{1,10}$ = .05, p = .829), benzodiazepine ($F_{1,10}$ = 2.75, p = .128) or antidepressant ($F_{1,10}$ = .82, p = .388) medications at the time of death, history of substance use disorder ($F_{1,10}$ = .11, p = .749), or manner of death ($F_{1,10}$ = .58, p = .464). In addition, the mean difference from their matched normal comparison subjects did not differ between MDD subjects with (n = 5) or without (n = 9) a history of psychosis ($F_{1,10}$ = .34, P = .575), suggesting that the lower density of ankyrin-G-IR AIS in the superficial zone of the subjects with schizophrenia reflects the disease process of schizophrenia and not a more general effect of psychosis.

The mean difference between matched pairs of schizophrenia and normal comparison subjects in the density of βIV spectrin-SD-IR AIS in the superficial zone did not significantly differ as a function of sex; antipsychotic, benzodiazepine or antidepressant medication use at time of death; history of substance use disorder; or manner of death (all F values < 1.15; all p values > .308). Similarly, no differences between matched pairs of MDD and normal comparison subjects in the density of βIV spectrin-SD-IR AIS in the superficial zone were found as a function of any of these factors (all F values < 1.64; all p values > .229).

Length of ankyrin-G- and βIV spectrin-SD-IR AIS

Because AIS length is associated with the probability that a given AIS will be contained, and identified, in a given tissue section, diagnosis-associated differences in the length of ankyrin-G- or βIV spectrin-SD-IR AIS could potentially confound our density measures. However, mean AIS length in the superficial cortical zone did not differ between normal comparison and schizophrenia subjects for either ankyrin-G ($F_{1,23} = 2.31$, $p = .14$) or βIV spectrin-SD ($F_{1,23} = 1.42$, $p = .25$).

Ankyrin-G-IR AIS in antipsychotic exposed monkeys

To further examine the potential effect of antipsychotic medications on ankyrin-G-IR AIS density, we determined the density of ankyrin-G-IR AIS in dlPFC area 46 of monkeys that had been exposed to haldoperidol, olanzapine or placebo (Fig. 7). As in humans, the density of labeled AIS was consistently greater in the superficial than in the deep cortical zone for each subject, but the mean density of ankyrin-G-IR AIS did not significantly differ across subject groups in either the superficial ($F_{2,14} = .29$, $p = .75$) or deep ($F_{2,14} = .49$, $p = .62$) zones.

Discussion

In this study, the density of ankyrin-G-IR AIS in subjects with schizophrenia was significantly reduced in the superficial, but not in the deep, cortical layers compared to both normal comparison and MDD subjects. This difference appears to reflect the underlying disease process of schizophrenia and not potential confounding factors. In contrast, the density of βIV spectrin-SD-IR AIS did not significantly differ across diagnostic groups in either the superficial or deep cortical layers.

Methodological considerations

We employed the stereological principle of systematic random sampling to reduce sampling bias. However, due to the unavailability of the entire dlPFC for all subjects, we report relative densities of labeled AIS instead of total numbers. This profile-counting approach is subject to two potential confounds. First, the detectability of labeled AIS is dependent upon their length and how much of that length is present in tissue sections; the latter is determined by the angle of cut of the tissue relative to the long axis of AIS. These issues do not appear to have confounded our results since the length of labeled AIS did not differ between the schizophrenia and normal comparion subject groups, and only locations in area 46 that were cut perpendicular to the pial surface, and parallel to the long axis of AIS, were sampled.

Second, the density of labeled AIS is dependent on both the number of AIS and cortical volume. However, systematic confounding due to differences in reference volume seems unlikely given that in these same subjects 1) previous measures of cortical thickness found no group differences (Pierri *et al* 1999), and 2) the densities of ankyrin-G-IR, βIV spectrin-SD–IR and $GABA_A$ receptor α2 subunit-IR (Volk *et al* 2002) AIS were decreased, unchanged and increased, respectively, in these subjects with schizophrenia relative to comparison subjects. Furthermore, if the volume of the dlPFC was reduced in the subjects with schizophrenia, as reported in some structural imaging studies (Shenton, *et al* 2001), then the lower density of ankyrin-G-IR AIS in schizophrenia observed in this study is likely to underestimate the true disease-related reduction in number of AIS with detectable levels of ankyrin-G immunoreactivity.

The densities of both ankyrin-G- and βIV spectrin-SD-IR AIS in the superficial layers differed as a function of sex, with females having greater densities in all subject groups (Figs. 3A and 4A). Interestingly, we previously did not find a difference in the densitities of ankyrin-G- or βIV spectrin-SD-IR AIS between male and female monkeys, or as a function of menstrual status in a small group of female monkeys (Cruz, *et al* 2008). Thus, whether the sex difference observed in the present study is distinctive to humans, and if so, the basis for it, requires further study.

None of the other factors examined (Fig. 6A) accounted for the lower density of ankyrin-G-IR AIS in the superficial zone of schizophrenia subjects, and no effects of typical or atypical antipsychotic medications on ankyrin-G-IR AIS density were observed in monkeys (Fig. 7). These findings, and the absence of a difference in ankyrin-G-IR AIS density between MDD and normal comparison subjects, or between MDD subjects with or without a history of psychosis, suggests that the lower density of ankyrin-G-IR AIS in the superficial zone of subjects with schizophrenia is specific to the disease process associated with this clinical diagnosis.

However, it is important to note that the gene that encodes ankyrin-G protein, ANK3, has recently been shown to be a susceptibility gene for bipolar disorder (Ferriera et al., 2008; Schulze et al., 2008). Given the evidence for shared genetic vulnerabilities between bipolar disorder and schizophrenia, it would be interesting to see if markers of GABA neurotransmission at the AIS of pyramidal neurons are altered in bipolar disorder. If genetic variants in the ANK3 gene also confer risk for schizophrenia, then these variants might contribute to reduced levels of ankyrin-G protein, but why such changes would be pronounced in a subset of pyramidal neurons is unclear.

Functional significance

The laminar specificity of the ankyrin-G-IR AIS findings are consistent with previous observations that pyramidal cell alterations in schizophrenia are more marked in the superficial cortical layers. For example, alterations in both pre- (i.e., lower density of GAT1-IR chandelier cell axon cartridges (Pierri, *et al* 1999)) and post- (i.e., higher density of AIS immunoreactive for the $GABA_A$ receptor α2 subunit (Volk, *et al* 2002)) synaptic markers of GABA inputs to pyramidal cell AIS are more prominent in the superficial than the deep layers of the dlPFC in schizophrenia. Similarly, smaller somal volume and lower spine

density of pyramidal neurons in schizophrenia are also preferentially found on layer 3 relative to layer 5-6 pyramidal neurons in both the dlPFC (Pierri, *et al* 2001; Glantz and Lewis, 2000; Kolluri, *et al* 2005; Rajkowska, *et al* 1998) and auditory cortex (Sweet, *et al* 2003; Sweet, *et al* 2004; Sweet, *et al* 2008). Because the majority of pyramidal neurons in dlPFC layers 2-3 project to other cortical areas (Jones, 1984), these lamina-specific alterations suggest a greater impact on cortical-cortical than on cortical-subcortical information processing in subjects with schizophrenia. Interestingly, in the superficial layers, the densities of AIS immunoreactive for ankyrin-G and for the $GABA_A$ receptor α2 subunit (Volk, *et al* 2002) were significantly inversely correlated in the schizophrenia subjects (r= -.690, p= .006) but not in the control subjects (r= -.229, p= .430). These findings suggest that a common factor may contribute to the changes in both ankyrin-G and the $GABA_A$ receptor α2 subunits at AIS in DLPFC layers 2-3 in subjects with schizophrenia. For example, if GABAergic innervation is required for the localization of ankyrin-G and the formation of the AIS (Hedstrom et al., 2008; Ango et al, 2004), then lower GABA neurotransmission from chandelier cells (due to a deficit in expression of the GABA synthesizing enzyme, GAD67 (Lewis et al., 2005)) to pyramidal cell AIS would be reflected in both decreased ankyrin-G and a compensatory increase in GABA receptors containing the α2 subunit. Similarly, the lower densities of both ankyrin-G- and βIV spectrin-SD-IR AIS in the deep relative to the superficial cortical zones might reflect the lower number of chandelier cell synapses on the AIS of pyramidal neurons in layer 6 relative to layer 3 (Farinas and DeFelipe, 1991). Fewer synaptic inputs might be associated with lower levels of immunoreactivity per AIS, creating the possibility that some AIS in the deep zone were not detected, and thus that diagnosis-related differences were missed.

The lower density of ankyrin-G-IR AIS in the superficial layers likely represents a reduced amount of ankyrin-G protein in a subset of AIS, rather than fewer AIS, for the following reasons. First, The density of βIV spectrin-SD-IR AIS was unchanged in schizophrenia, and exceeded the density of ankyrin-G-IR AIS in every subject, including controls, indicating that AIS are still present in schizophrenia. The consistent difference in the densities of ankyrin-G-IR and βIV spectrin-SD-IR AIS might merely reflect a greater sensitivity of βIV spectrin-SD antibody. Thus, our findings suggest that in schizophrenia a subset of pyramidal neuron AIS have reduced levels of ankyrin-G protein such that they are no longer detectable by immunocytochemistry while the reduced levels of βIV spectrin in these AIS is still sufficient to be detected. Second, both the total number of prefrontal neurons (Thune, *et al* 2001), and the tissue shrinkage-corrected density of layer 3 pyramidal neurons (Maldonado-Aviles, *et al* 2006), are unchanged in subjects with schizophrenia, indicating that the source neurons of AIS are still present.

Although both ankyrin-G and βIV spectrin play roles in the formation and maintenance of the membrane protein complexes that comprise the AIS, ankyrin-G appears to be the principal organizer of the AIS. For example, in ankyrin-G knock-out mice, βIV spectrin, as well as sodium and potassium ion channels, fail to cluster at the AIS of Purkinje neurons (Zhou, *et al* 1998; Bennett and Baines, 2001; Pan, *et al* 2006). In contrast, ankyrin-G is properly localized to the AIS in βIV spectrin knock-out mice (Yang, *et al* 2004) and βIV spectrin by itself cannot recruit proteins, such as sodium channels, to the AIS (Yang, *et al*

2007). Thus, lower levels of ankyrin-G protein in schizophrenia may translate into a deficit in the levels of sodium channels localized to the AIS, and consequently to a reduced capacity of layer 2-3 pyramidal neurons to generate action potentials. Ankyrin-G also localizes and retains the cell adhesion molecule, neurofascin 186, to the AIS of projection neurons (Ango, *et al* 2004; Boiko, *et al* 2007). Through its interaction with ankyrin-G, neurofascin 186 is responsible for the recruitment of GABA synapses to the AIS of cerebellar purkinje neurons (Ango, *et al* 2004). If this same mechanism is operative in cortical pyramidal neurons, then lower levels of ankyrin-G could lead to a smaller number of GABA synapses at the AIS of layer 2-3 pyramidal neurons in schizophrenia. These hypotheses may be tested in future studies by examining immunoreactivity for voltage-gated sodium channels and neurofascin 186 in the AIS of subjects with schizophrenia.

The combination of lower synaptic input from chandelier neurons and impaired action potential generation could disrupt the capacity of pyramidal neurons to fire in the repetitive and synchronous fashion required for cortical network oscillations, such as those in the gamma band (30-80 Hz) range (Gonzalez-Burgos and Lewis, 2008). Prefrontal gamma oscillations are associated with certain cognitive processes, such as working memory, that are disturbed in schizophrenia, and cognitive task-induced gamma oscillations in the frontal lobes are reduced in schizophrenia (Cho, *et al* 2006). Although additional studies are required to determine the cause-effect relationships between alterations at the site of chandelier-pyramidal neuron synapses, the findings of the present study further define the molecular nature of those alterations and may suggest novel targets for therapeutic interventions.

Acknowledgments

Supported by NIH grants MH043784, MH045156 and MH084053 from the National Institute of Mental Health. The content is solely the responsibility of the authors and does not necessarily represent the official views of the National Institute of Mental Health or the National Institutes of Health. The authors thank Dr. Matthew Rasband for providing the βIV spectrin antibody, Mary Brady for excellent assistance with the figures, Lindsay Karr for preparing the manuscript, and the members of the Clinical Services and Diagnostics Core of the Conte Center for the Neuroscience of Mental Disorders (MH084053) for their assistance in diagnostic assessments.

References

Akbarian S, Huntsman MS, Kim JJ, Tafazzoli A, Potkin SG, Bunney WE Jr, Jones EG. $GABA_A$ receptor subunit gene expression in human prefrontal cortex: Comparison of schizophrenics and controls. Cereb Cortex. 1995; 5:550–560. [PubMed: 8590827]

Ango F, Di Cristo G, Higashiyama H, Bennett V, Wu P, Huang ZJ. Ankyrin-based subcellular gradient of neurofascin, an immunoglobulin family protein, directs GABAergic innervation at purkinje axon initial segment. Cell. 2004; 119:257–272. [PubMed: 15479642]

Bennett V, Baines AJ. Spectrin and ankyrin-based pathways: Metazoan inventions for integrating cells into tissues. Physiol Rev. 2001; 81:1353–1392. [PubMed: 11427698]

Boiko T, Vakulenko M, Ewers H, Yap CC, Norden C, Winckler B. Ankyrin-dependent and -independent mechanisms orchestrate axonal compartmentalization of L1 family members neurofascin and L1/neuron-glia cell adhesion molecule. J Neurosci. 2007; 27:590–603. [PubMed: 17234591]

Cho RY, Konecky RO, Carter CS. Impairments in frontal cortical gamma synchrony and cognitive control in schizophrenia. Proc Natl Acad Sci U S A. 2006; 103:19878–19883. [PubMed: 17170134]

Cruz DA, Eggan SM, Lewis DA. Postnatal development of pre- and post-synaptic GABA markers at chandelier cell inputs to pyramidal neurons in monkey prefrontal cortex. J Comp Neurol. 2003; 465:385–400. [PubMed: 12966563]

Cruz DA, Lovallo EM, Stockton S, Rasband M, Lewis DA. Postnatal development of synaptic structure proteins in pyramidal neuron axon initial segments in monkey prefrontal cortex. J Comp Neurol. 2008 in press.

Daviss SR, Lewis DA. Local circuit neurons of the prefrontal cortex in schizophrenia: Selective increase in the density of calbindin-immunoreactive neurons. Psychiatry Res. 1995; 59:81–96. [PubMed: 8771223]

Dorph-Petersen K-A, Pierri JN, Perel JM, Sun Z, Sampson AR, Lewis DA. The influence of chronic exposure to antipsychotic medications on brain size before and after tissue fixation: A comparison of haloperidol and olanzapine in macaque monkeys. Neuropsychopharm. 2005; 30:1649–1661.

Erickson SL, Akil M, Levey AI, Lewis DA. Postnatal development of tyrosine hydroxylase- and dopamine transporter-immunoreactive axons in monkey rostral entorhinal cortex. Cereb Cortex. 1998; 8:415–427. [PubMed: 9722085]

Farinas I, DeFelipe J. Patterns of synaptic input on corticocortical and corticothalamic cells in the cat visual cortex. II. The axon initial segment. J Comp Neurol. 1991; 304:70–77. [PubMed: 2016413]

Glantz LA, Lewis DA. Reduction of synaptophysin immunoreactivity in the prefrontal cortex of subjects with schizophrenia: Regional and diagnostic specificity. Arch Gen Psychiatry. 1997; 54:943–952. [PubMed: 9337775]

Glantz LA, Lewis DA. Decreased dendritic spine density on prefrontal cortical pyramidal neurons in schizophrenia. Arch Gen Psychiatry. 2000; 57:65–73. [PubMed: 10632234]

Gonzalez-Burgos G, Lewis DA. GABA neurons and the mechanisms of network oscillations: implications for understanding cortical dysfunction in schizophrenia. Schizophr Bull. 2008; 34:944–961. [PubMed: 18586694]

Guidotti A, Auta J, Davis JM, Gerevini VD, Dwivedi Y, Grayson DR, Impagnatiello F, Pandey G, Pesold C, Sharma R, Uzunov D, et al. Decrease in reelin and glutamic acid decarboxylase$_{67}$ (GAD$_{67}$) expression in schizophrenia and bipolar disorder. Arch Gen Psychiatry. 2000; 57:1061–1069. [PubMed: 11074872]

Hashimoto T, Arion D, Unger T, Maldonado-Aviles JG, Morris HM, Volk DW, Mirnics K, Lewis DA. Alterations in GABA-related transcriptome in the dorsolateral prefrontal cortex of subjects with schizophrenia. Mol Psychiatry. 2008; 13:147–161. [PubMed: 17471287]

Hashimoto T, Volk DW, Eggan SM, Mirnics K, Pierri JN, Sun Z, Sampson AR, Lewis DA. Gene expression deficits in a subclass of GABA neurons in the prefrontal cortex of subjects with schizophrenia. J Neurosci. 2003; 23:6315–6326. [PubMed: 12867516]

Jenkins SM, Bennett V. Ankyrin-G coordinates assembly of the spectrin-based membrane skeleton, voltage-gated sodium channels, and L1 CAMs at Purkinje neuron initial segments. J Cell Biol. 2001; 155:739–745. [PubMed: 11724816]

Jenkins SM, Bennett V. Developing nodes of Ranvier are defined by ankyrin-G clustering and are independent of paranodal axoglial adhesion. Proc Natl Acad Sci U S A. 2002; 99:2303–2308. [PubMed: 11842202]

Jenkins SM, Kizhatil K, Kramarcy NR, Sen A, Sealock R, Bennett V. FIGQY phosphorylation defines discrete populations of L1 cell adhesion molecules at sites of cell-cell contact and in migrating neurons. Journal of Cell Science. 2001; 114:3823–3835. [PubMed: 11719549]

Jiao Y, Sun Z, Lee T, Fusco FR, Kimble TD, Meade CA, Cuthbertson S, Reiner A. A simple and sensitive antigen retrieval method for free-floating and slide-mounted tissue sections. J Neurosci Meth. 1999; 93:149–162.

Jones, EG. Laminar distribution of cortical efferent cells. In: Peters, A.; Jones, EG., editors. Cerebral Cortex. Vol. 1. Plenum Press; New York: 1984. p. 521-553.

Kolluri N, Sun Z, Sampson AR, Lewis DA. Lamina-specific reductions in dendritic spine density in the prefrontal cortex of subjects with schizophrenia. Am J Psychiatry. 2005; 162:1200–1202. [PubMed: 15930070]

Kordeli E, Lambert S, Bennett V. AnkyrinG. A new ankyrin gene with neural-specific isoforms localized at the axonal initial segment and node of Ranvier. J Biol Chem. 1995; 270:2352–2359. [PubMed: 7836469]

Lacas-Gervais S, Guo J, Strenzke N, Scarfone E, Kolpe M, Jahkel M, De Camilli P, Moser T, Rasband MN, Solimena M. BetaIVSigma1 spectrin stabilizes the nodes of Ranvier and axon initial segments. J Cell Biol. 2004; 166:983–990. [PubMed: 15381686]

Lewis DA, Campbell MJ, Foote SL, Morrison JH. The monoaminergic innervation of primate neocortex. Human Neurobiol. 1986; 5:181–188.

Lewis DA, Hashimoto T, Volk DW. Cortical inhibitory neurons and schizophrenia. Nat Rev Neurosci. 2005; 6:312–324. [PubMed: 15803162]

Maldonado-Aviles JG, Wu Q, Sampson AR, Lewis DA. Somal size of immunolabeled pyramidal cells in the prefrontal cortex of subjects with schizophrenia. Biol Psychiatry. 2006; 60:226–234. [PubMed: 16460698]

Melchitzky DS, Sesack SR, Lewis DA. Parvalbumin-immunoreactive axon terminals in macaque monkey and human prefrontal cortex: Laminar, regional and target specificity of Type I and Type II synapses. J Comp Neurol. 1999; 408:11–22. [PubMed: 10331577]

Ohnuma T, Augood SJ, Arai H, McKenna PJ, Emson PC. Measurement of GABAergic parameters in the prefrontal cortex in schizophrenia: Focus on GABA content, $GABA_A$ receptor α-1 subunit messenger RNA and human GABA transporter-1 (HGAT-1) messenger RNA expression. Neuroscience. 1999; 93:441–448. [PubMed: 10465426]

Pan ZM, Kao TC, Horvath Z, Lemos J, Sul JY, Cranstoun SD, Bennett V, Scherer SS, Cooper EC. A common ankyrin-G-based mechanism retains KCNQ and Na-V channels at electrically active domains of the axon. J Neurosci. 2006; 26:2599–2613. [PubMed: 16525039]

Pierri JN, Chaudry AS, Woo T-U, Lewis DA. Alterations in chandelier neuron axon terminals in the prefrontal cortex of schizophrenic subjects. Am J Psychiatry. 1999; 156:1709–1719. [PubMed: 10553733]

Pierri JN, Volk CLE, Auh S, Sampson A, Lewis DA. Decreased somal size of deep layer 3 pyramidal neurons in the prefrontal cortex of subjects with schizophrenia. Arch Gen Psychiatry. 2001; 58:466–473. [PubMed: 11343526]

Pucak ML, Levitt JB, Lund JS, Lewis DA. Patterns of intrinsic and associational circuitry in monkey prefrontal cortex. J Comp Neurol. 1996; 376:614–630. [PubMed: 8978474]

Rajkowska G, Goldman-Rakic PS. Cytoarchitectonic definition of prefrontal areas in the normal human cortex: I. Remapping of areas 9 and 46 using quantitative criteria. Cereb Cortex. 1995; 5:307–322. [PubMed: 7580124]

Rajkowska G, Selemon LD, Goldman-Rakic PS. Neuronal and glial somal size in the prefrontal cortex: A postmortem morphometric study of schizophrenia and Huntington disease. Arch Gen Psychiatry. 1998; 55:215–224. [PubMed: 9510215]

Shenton ME, Dickey CC, Frumin M, McCarley RW. A review of MRI findings in schizophrenia. Schizophr Res. 2001; 49:1–52. [PubMed: 11343862]

Susuki K, Rasband MN. Spectrin and ankyrin-based cytoskeletons at polarized domains in myelinated axons. Exp Biol Med (Maywood). 2008; 233:394–400. [PubMed: 18367627]

Sweet RA, Bergen SE, Sun Z, Sampson AR, Pierri JN, Lewis DA. Pyramidal cell size reduction in schizophrenia: Evidence for involvement of auditory feedforward circuits. Biol Psychiatry. 2004; 55:1128–1137. [PubMed: 15184031]

Sweet RA, Henteleff RA, Zhang W, Sampson AR, Lewis DA. Reduced dendritic spine density in auditory cortex of subjects with schizophrenia. Neuropsychopharm. 2008 Epub May 7, 2008.

Sweet RA, Pierri JN, Auh S, Sampson AR, Lewis DA. Reduced pyramidal cell somal volume in auditory association cortex of subjects with schizophrenia. Neuropsychopharm. 2003; 28:599–609.

Thune JJ, Uylings HBM, Pakkenberg B. No deficit in total number of neurons in the prefrontal cortex in schizophrenics. J Psychiatr Res. 2001; 35:15–21. [PubMed: 11287052]

Volk DW, Austin MC, Pierri JN, Sampson AR, Lewis DA. Decreased glutamic acid decarboxylase67 messenger RNA expression in a subset of prefrontal cortical gamma-aminobutyric acid neurons in subjects with schizophrenia. Arch Gen Psychiatry. 2000; 57:237–245. [PubMed: 10711910]

Volk DW, Austin MC, Pierri JN, Sampson AR, Lewis DA. GABA transporter-1 mRNA in the prefrontal cortex in schizophrenia: Decreased expression in a subset of neurons. Am J Psychiatry. 2001; 158:256–265. [PubMed: 11156808]

Volk DW, Pierri JN, Fritschy J-M, Auh S, Sampson AR, Lewis DA. Reciprocal alterations in pre- and postsynaptic inhibitory markers at chandelier cell inputs to pyramidal neurons in schizophrenia. Cereb Cortex. 2002; 12:1063–1070. [PubMed: 12217970]

Williams SM, Goldman-Rakic PS, Leranth C. The synaptology of parvalbumin-immunoreactive neurons in primate prefrontal cortex. J Comp Neurol. 1992; 320:353–369. [PubMed: 1613130]

Woo T-U, Whitehead RE, Melchitzky DS, Lewis DA. A subclass of prefrontal gamma-aminobutyric acid axon terminals are selectively altered in schizophrenia. Proc Natl Acad Sci U S A. 1998; 95:5341–5346. [PubMed: 9560277]

Yang Y, Lacas-Gervais S, Morest DK, Solimena M, Rasband MN. BetaIV spectrins are essential for membrane stability and the molecular organization of nodes of Ranvier. J Neurosci. 2004; 24:7230–7240. [PubMed: 15317849]

Yang Y, Ogawa Y, Hedstrom KL, Rasband MN. beta IV spectrin is recruited to axon initial segments and nodes of Ranvier by ankyrinG. J Cell Biol. 2007; 176:509–519. [PubMed: 17283186]

Zhou DX, Lambert S, Malen PL, Carpenter S, Boland LM, Bennett V. Ankyrin(G) is required for clustering of voltage-gated Na channels at axon initial segments and for normal action potential firing. J Cell Biol. 1998; 143:1295–1304. [PubMed: 9832557]

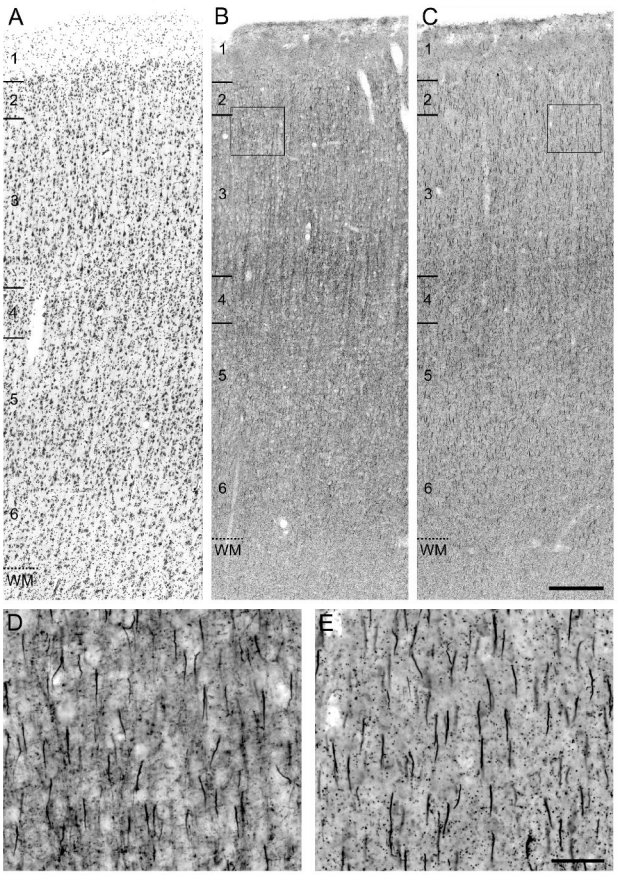

Figure 1.

Brightfield photomicrographs of a Nissl-stained section (A) demonstrating the normal cytoarchitecture of human dlPFC area 46 and of adjacent sections labeled for ankyrin-G (B) and βIV spectrin-SD (C) immunoreactivity. Numerals indicate cortical layers and the dashed line represents the layer 6 - white matter (WM) border. Boxes in B and C approximate the location of higher power photomicrographs in D and E, which show the AIS of pyramidal neurons immunoreactive for ankyrin G (D) and βIV spectrin-SD, as well as punctate labeling for each marker which likely represents nodes of Ranvier. Scale bars = 300 μm (A-C); 50 μm (D, E).

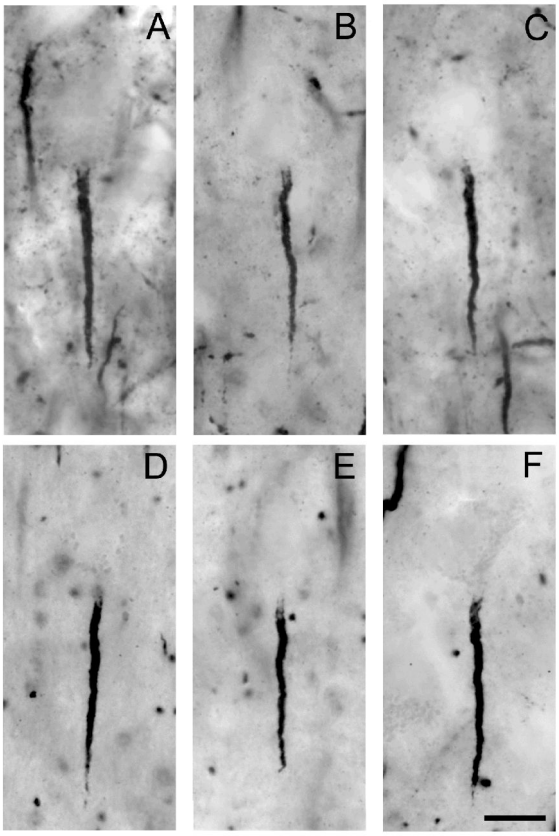

Figure 2.

Brightfield photomicrographs of representative pyramidal neuron AIS in the superficial zone of dlPFC area 46 immunoreactive for ankyrin-G (A, B, C) or βIV spectrin-SD (D, E, F) in control subjects (A, D), schizophrenia subjects (B,E), and MDD subjects (C,F). Scale bar = 10 μm (A - F).

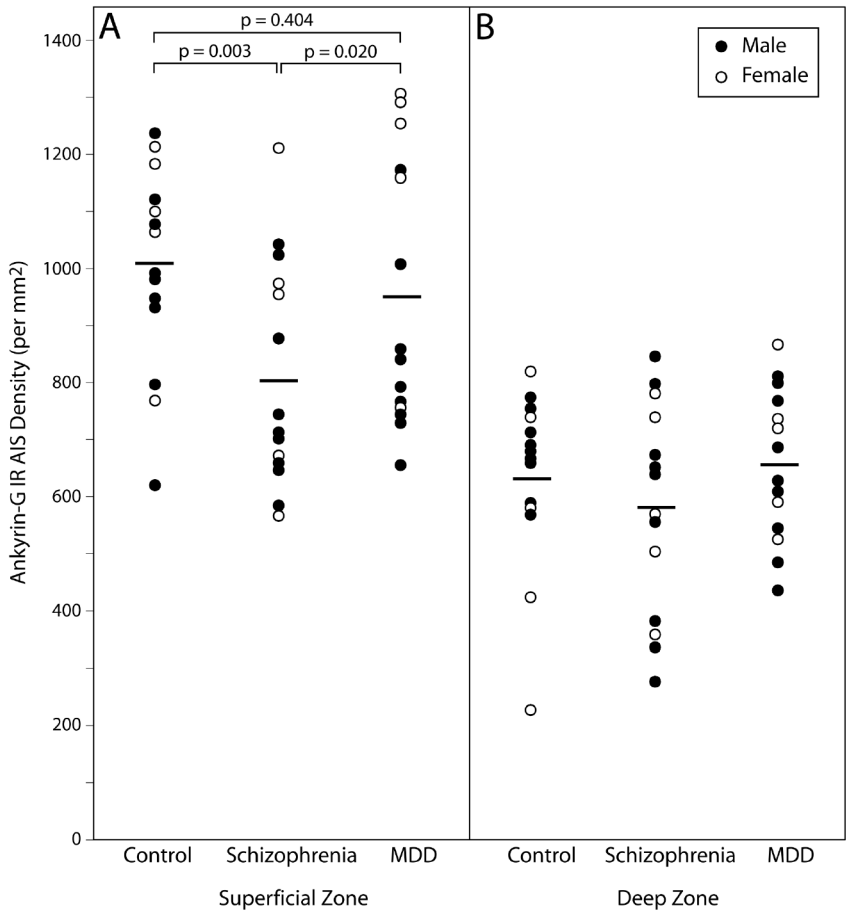

Figure 3.

Scatter plots showing the mean densities of ankyrin-G immunoreactive AIS in each subject for each cortical zone. Horizontal lines indicate the mean density for each group. Note the generally higher density of ankyrin-G-labeled AIS for female subjects in the superficial zone.

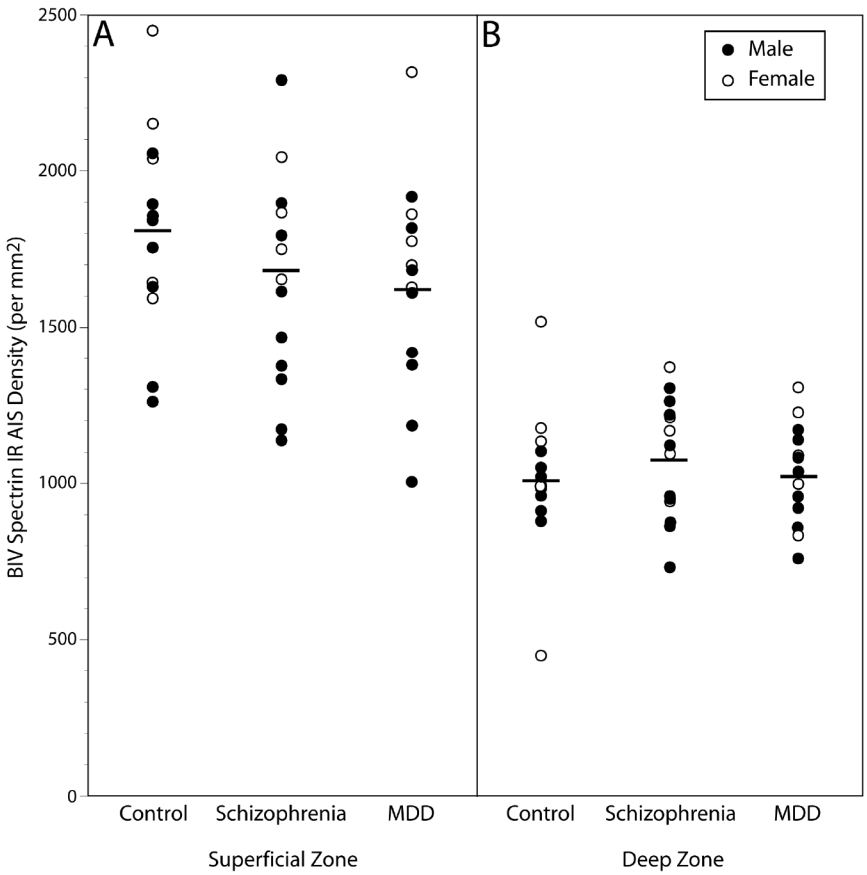

Figure 4.

Scatter plots showing the mean densities of βIV spectrin-SD immunoreactive AIS in each subject for each cortical zone. Horizontal lines indicate the mean density for each group. Note the generally higher density of βIV spectrin-SD immunoreactive AIS for female subjects in the superficial zone.

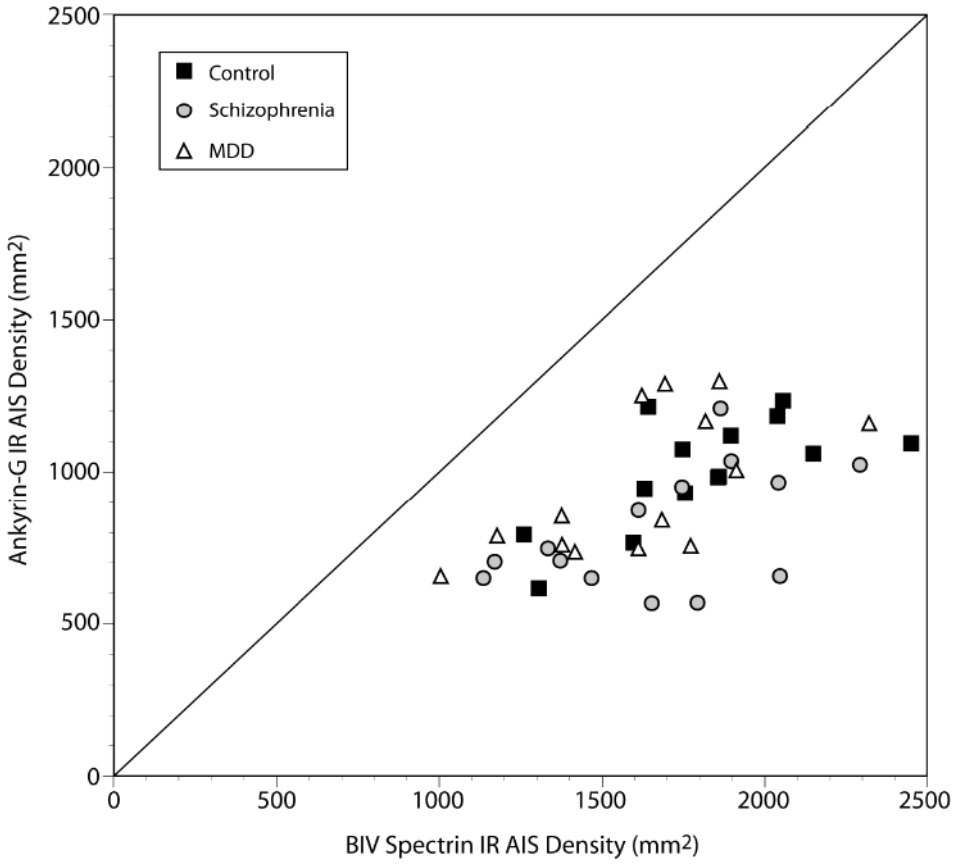

Figure 5.

Scatter plot showing the relationship between ankyrin-G- and βIV spectrin-SD-immunoreactive AIS density in the superficial cortical zone for each subject. All values fall below the unity line indicating a greater density of βIV spectrin-SD-immunoreactive AIS in every subject.

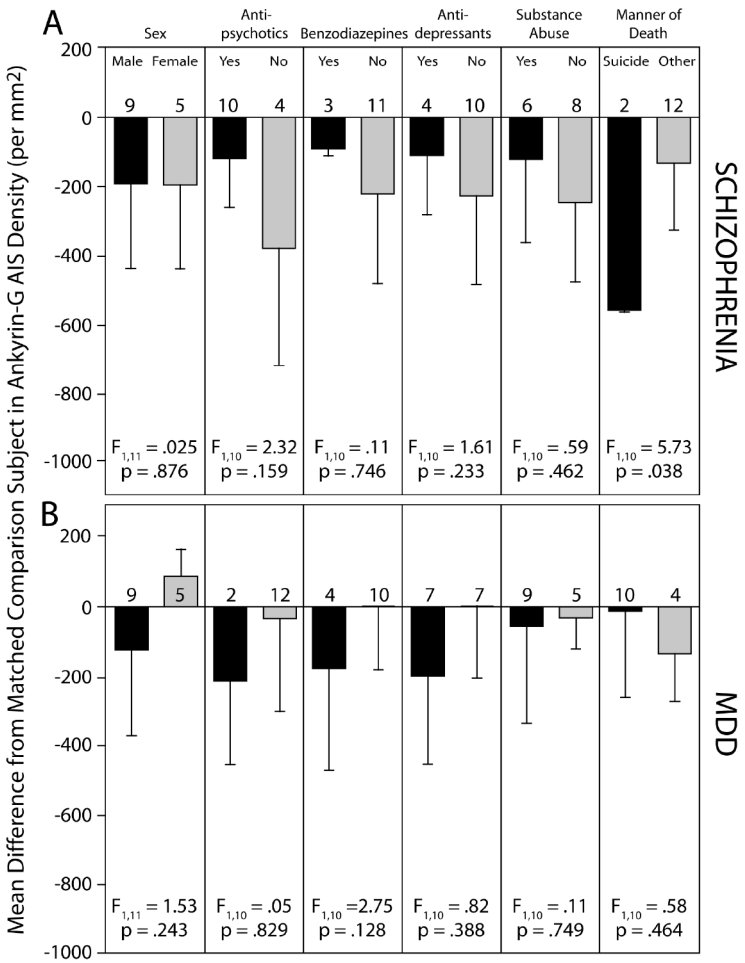

Figure 6.

Bar graphs showing the mean (±SD) difference from the matched normal comparison subject for ankyrin-G immunoreactive AIS density in the superficial zone for schizophrenia (panel A) and MDD (panel B) groups. Schizophrenia and MDD subjects are separated into groups according to sex; use of antipsychotics, benzodiazepines, or antidepressants at time of death; history of substance use disorder; and manner of death. Numbers at the origin line indicate the number of subjects in each group.

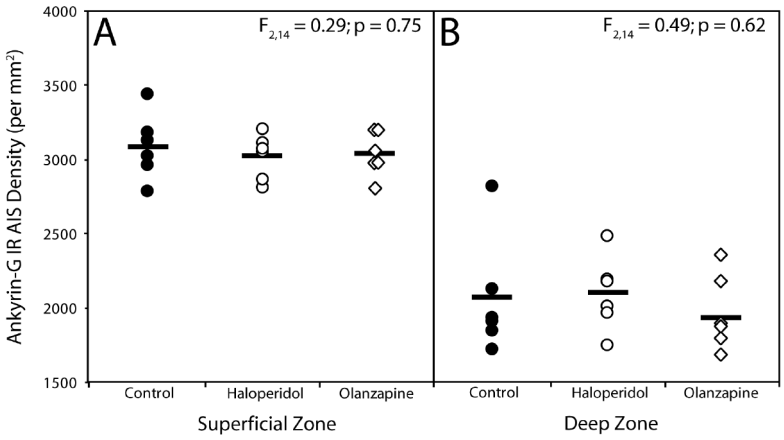

Figure 7.

Scatter plots showing the mean densities of ankyrin-G-IR AIS in each subject for each cortical zone in placebo-, haloperidol- and olanzapine-exposed monkeys. Horizontal lines indicate the mean density for each group.

Table 1

Subject Characteristics

Subject Group[1]		Case No.	S/A[2]	PMI[3]	ST[4]	Cause of death[5]	*DSM IV* diagnoses[6] Primary	Substance	Meds ATOD[7]
1	C	250	F/47	5.3	174	ASCVD	N		N
	S	398	F/41	10.3	150	Pulmonary embolus	SA		B; P
	M	210	F/50	4.7	181	Suicide by drowning	MDD		N
2	C	270	M/62	3.3	171	ASCVD	N		N
	S	131	M/62	3.9	197	Pneumonia	US	AAR	P
	M	249	M/57	4.3	174	ASCVD	MDDpf		N
3	C	451	M/48	12.0	133	ASCVD	N		N
	S	317	M/48	8.3	164	Pneumonia	US		D; P
	M	511	M/34	17.9	119	ASCVD	MDD		N
4	C	178	M/48	7.8	184	ASCVD	N		N
	S	377	M/25	10.0	156	GI Bleeding	US	ADC	P
	M	505	M/57	12.8	121	Suicide by gunshot	MD	ADC	N
5	C	420	F/67	19.5	144	Accidental CO intoxication	N		N
	S	333	F/66	17.9	163	ASCVD	US		D; P
	M	803	F/65	18.0	74	Trauma	MDD		P
6	C	344	M/50	6.8	161	ASCVD	N		N
	S	422	M/54	11.0	144	ASCVD	PS		B; P
	M	698	M/59	13.0	93	Suicide by hanging	MDDpf		D; P
7	C	449	F/47	4.3	134	Accidental CO intoxication	N		N
	S	517	F/48	3.7	119	Intracerebral hemorrhage	DS	ADC	P
	M	248	F/48	6.3	174	Suicide by hanging	MDD	OAC	B; D
8	C	412	M/42	14.2	148	Aortic stenosis	N		N
	S	466	M/48	19.0	131	ASCVD	US		P
	M	421	M/44	16.0	144	ASCVD	MDD	AAR	N

Neuropsychopharmacology. Author manuscript; available in PMC 2010 February 01.

Subject Group[1]		Case No.	S/A[2]	PMI[3]	ST[4]	Cause of death[5]	*DSM IV* diagnoses[6] Primary	Substance	Meds ATOD[7]
9	C	592	M/41	22.1	108	ASCVD	N		N
	S	450	M/48	22.0	134	Suicide by jumping	US	ADR; ODR	N
	M	689	M/45	24.4	94	Suicide by acid ingestion	MDDpf	AAR	B; D; P
10	C	681	M/51	11.6	95	Cardiomyopathy	N		N
	S	234	M/51	12.8	177	Cardiomyopathy	PS		P
	M	602	M/56	11.8	106	Suicide by gunshot	MDD	ADC	N
11	C	567	F/46	15.0	112	Mitral valve prolapse	N		N
	S	537	F/37	14.5	117	Suicide by hanging	SA		N
	M	693	F/42	12.6	94	Suicide by overdose	MDDpf	ODC	B; D
12	C	568	F/60	9.5	112	ASCVD	N		N
	S	559	F/61	16.8	113	ASCVD	SA	ADC	D; P
	M	565	F/62	12.4	112	Suicide by gunshot	MDD	AAC; ODR	D
13	C	620	M/64	17.3	103	Accidental drowning	N		N
	S	566	M/63	18.3	112	ASCVD	US	AAR	B; D; P
	M	613	M/59	15.6	104	Suicide by gunshot	MDDpf	AAR	N
14	C	551	M/61	16.4	114	Cardiac tamponade	N		N
	S	622	M/58	18.9	103	Right MCA infarction	US		N
	M	619	M/55	18.8	103	Suicide by gunshot	MDD	ODR	B; D

Abbreviations by column:

[1] C, normal comparison; S, schizophrenia; M, mood disorder;

[2] A, age in years; F, female; M, male; S, sex;

[3] PMI, postmortem interval;

[4] ST, storage time in months at -80°C;

[5] ASCVD, atherosclerotic cardiovascular disease; CO, carbon monoxide; COPD, chronic obstructive pulmonary disease; OD, overdose;

[6] pf, psychotic features; DS, disorganized schizophrenia; PS, paranoid schizophrenia; SA, schizoaffective disorder; US, undifferentiated schizophrenia; AAC, alcohol abuse, current at time of death; AAR, alcohol abuse, in remission at time of death; ADC, alcohol dependence, current at time of death; ADR, alcohol dependence, in remission at time of death; MD-M, mood disorder due to a general medical condition; MDD, major depressive disorder; ODC, other substance dependence, current at time of death; ODR, other substance dependence, in remission at time of death; OAC, other substance abuse, current at time of death; OAR, other substance abuse, in remission at time of death;

[7] Meds ATOD, medications at time of death; B, benzodiazepines; D, antidepressants; N, none; P, antipsychotics.